ResearchGate

See discussions, stats, and author profiles for this publication at: https://www.researchgate.net/publication/230275432

Polymerization of ethylene by (α-Diimine) nickel catalyst and statistical analysis of the effects of reaction conditions

ARTICLE *in* POLYMER ENGINEERING AND SCIENCE · SEPTEMBER 2010

Impact Factor: 1.52 · DOI: 10.1002/pen.21704

CITATIONS
6

READS
28

6 AUTHORS, INCLUDING:

Geraldo L. Crossetti
Universidade Federal do Pampa (Unipampa)
18 PUBLICATIONS **120** CITATIONS
SEE PROFILE

Griselda Barrera Galland
Universidade Federal do Rio Grande do Sul
97 PUBLICATIONS **1,647** CITATIONS
SEE PROFILE

Marcio Nele
Federal University of Rio de Janeiro
112 PUBLICATIONS **914** CITATIONS
SEE PROFILE

Available from: Griselda Barrera Galland
Retrieved on: 24 January 2016

Polymerization of Ethylene by (α-Diimine) Nickel Catalyst and Statistical Analysis of the Effects of Reaction Conditions

Luis Carlos Ferreira Jr.,[1] Priamo Albuquerque Melo Jr.,[1] Geraldo Lopes Crossetti,[2] Griselda Barrera Galland,[3] Marcio Nele,[4] José Carlos Pinto[1]

[1] *Programa de Engenharia Química/COPPE, Universidade Federal do Rio de Janeiro, Cidade Universitária, CP: 68502, Rio de Janeiro, 21945-970 RJ, Brazil*

[2] *Escola de Química - Universidade Federal do Rio de Janeiro, Rio de Janeiro, RJ, Brazil*

[3] *Departamento de Química e Física - Universidade de Santa Cruz, Santa Crus do Sul, RS, Brazil*

[4] *Instituto de Química - Universidade Federal do Rio Grande do Sul, Porto Alegre, RS, Brazil*

This article regards the ethylene polymerization catalyzed by a nickel catalyst and activated by ethylaluminum sesquichloride (EASC). The effects of the reaction conditions [polymerization temperature, cocatalyst (EASC) concentration, and ethylene concentration] on the average molecular weights of the final polymers and reaction yields were evaluated with the help of empirical statistical models. It is shown that reaction temperature and cocatalyst (EASC) concentration exert the most important effects on average molecular weights and catalyst activity. The polydispersities of the obtained polyethylenes are larger than the polydispersities of polyethylenes obtained with typical Brookhart catalysts. The analysis of polymer branching frequencies shows new types of short branching and significant amounts of long branches, which may explain the relatively large polydispersities of the obtained polymer samples. POLYM. ENG. SCI., 50:1797–1808, 2010.
© 2010 Society of Plastics Engineers

INTRODUCTION

The investigation of short chain branching in linear low-density polyethylenes (LLDPE) and of long chain branching in low-density polyethylenes (LDPE) has gained increasing importance over the last decade. This is because of the growing importance of these polymer materials, which present outstanding mechanical properties, resulting from the branched structures placed along the polymer backbone. Although flow properties and overall polymer-processing behavior are largely influenced by the molecular weight distribution, the existence of branched structures and the respective branching distributions also exert important effects on the operation of film-blowing processes, as a consequence of the modification of the solidification and crystallization properties of the blown film. This is due to modification of the crystallization kinetics of LLDPE and LDPE, which depends on existence of branched structures and their distribution along the polymer chain. Therefore, branching is of paramount importance for proper understanding of the processing behavior of both LLDPE and LDPE [1–3].

The production of polyolefins is usually performed commercially with Ziegler-Natta catalysts. These catalysts are used to promote ethylene or α-olefins copolymerization reactions and to produce polymers with short-chain branches. These copolymers present random distributions of short branches along the polymer backbone, as a consequence of the polymerization mechanism, and broad molecular weight distribution, due to the existence of multiple active catalyst sites. These characteristics lead to polymer materials with inferior mechanical properties, when compared with polymers produced with metallocene catalysts [4]. Metallocene catalysts allow for production of distinct copolymers, with properties ranging from those of high-density linear polyethylene (HDPE) to those of LLDPE, due to the improved control of the polymer structure attained with these catalysts [1–4].

Correspondence to: José Carlos Pinto; e-mail: pinto@peq.coppe.ufrj.br
Contract grant sponsors: CNPq (Conselho Nacional de Desenvolvimento Científico e Tecnológico), FAPERJ (Fundação Carlos Chagas Filho de Apoio à Pesquisa do Estado do Rio de Janeiro), Suzano Petroquímica SA, Petroflex SA.
DOI 10.1002/pen.21704
View this article online at wileyonlinelibrary.com.
© 2010 Society of Plastics Engineers

Long chain branching does not occur (or occur marginally) when conventional Ziegler-Natta catalysts are used to perform low-pressure polymerizations. However, some metallocene catalysts are able to incorporate long chain branches into the polymer chain even at low pressures [3]. For example, Kolodka et al. [5] and Beigzadeh et al. [6–8] have reported the production of long chain branched polymers with the "constrained geometry catalyst" (CGC). Kolodka et al. [9] and Malmberg et al. [10, 11] reported the incorporation of long chain branches into polyethylene chains with various metallocene catalysts. According to Carlini et al. [12], it is possible to obtain long chain–branched polyethylenes even with the well-known metallocene catalyst Cp_2ZrCl_2.

To produce long chain–branched polyolefins, it is normally assumed that the catalyst systems must be able to perform at least two distinct reaction steps. First, the catalyst must be able to produce vinyl-terminated polymer chains through spontaneous chain transfer. These unsaturated polymer chains can be regarded as macromonomers that can be incorporated into growing polymer chains. Second, the catalyst must be able to promote the insertion of these macromonomers into the growing polymer chains. In this case, both the catalyst system and the polymerization conditions are very important for obtaining polymers with long-chain branches [5].

In the last few years, very versatile late transition metal catalysts have been developed for ethylene polymerization [13–15]. Such catalysts enable the formation of short-branched polymers without usage of comonomers. In general, these catalysts contain a multidentade ligand that coordinates the late transition metal atom through nitrogen, oxygen, or phosphorous atoms [13–21]. The late transition metals that are active for olefin polymerizations are Ni, Co, and Fe. Depending on the ligands, different types of polyolefins can be obtained, from HDPE to LLDPE [13–21]. It has also been observed that these catalysts are able to produce long chain branches through macromonomer reincorporation. This discovery opened new possibilities for production of polyolefins with short- and long-chain branches in the polyethylene chain simultaneously [19]. As a result, efforts have been made to understand how polymerization conditions influence the properties of materials prepared with these catalyst systems [12, 13].

Cocatalysts that activate the late transition complexes for polymerization have been studied, and it is known that some alkylaluminum halides are able to activate these complexes as effectively as methylaluminoxane (MAO). Nickel diimine complexes can be activated prior to use as polymerization catalysts. Ordinary alkyl aluminum, such as diethyl aluminum chloride (DEAC), can promote ethylene polymerization with [η^3-methallyl-nickel-diimine]PF_6, allowing for replacement of MAO as the cocatalyst [22]. Svejda et al. showed that DEAC or (α-diimine) nickel complexes can produce polyethylenes with longer chains than polyethylenes obtained with MAO [23]. Maldanis et al. showed that alkylaluminum, DEAC, and alkylaluminoxanes halides (DCDAO) can activate nickel (Ni) catalysts with the same efficiency of MAO [24]. As ordinary alkylaluminum compounds are much cheaper and can be handled much easier than MAO, there are incentives for using ordinary alkylaluminum compounds as cocatalysts.

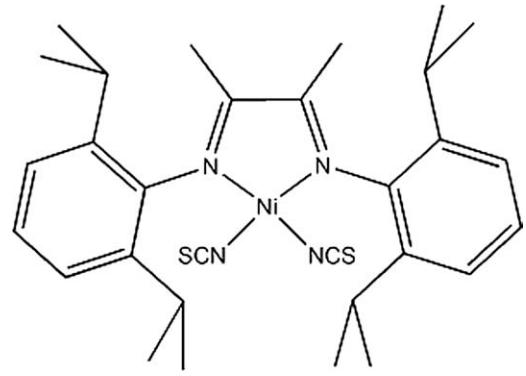

FIG. 1. (α-diimine) nickel catalyst used to perform ethylene polymerizations.

The main objective of this work is to investigate the polymerization of ethylene, based on the previous remarks, with a nickel (α-diimine) complex activated by ethylaluminum sesquichloride (EASC). The catalyst of interest has been synthesized by one of the authors and is described in detail elsewhere [25]. Figure 1 shows the catalyst structure, as presented in the original reference (see Fig. 1). The cocatalyst was selected in accordance with a preliminary investigation performed to replace MAO for an alternative and cheaper cocatalyst [26]. The effects of the reaction conditions (polymerization temperature, cocatalyst (EASC) concentration and ethylene concentration) on the molecular weight distributions of final polymer materials and on the reaction yields are evaluated with the help of empirical statistical models. In addition, the analysis of polymer branching shows new branch structures that had not been described before.

EXPERIMENTAL PART

Reagents

The Ni (II) complex was synthesized as described elsewhere [25] and manipulated under nitrogen atmosphere with standard Schlenk techniques. Ethylene (99.8%) and nitrogen (99.5%) were purchased from AGA (Rio de Janeiro, Brazil). Gaseous feed streams were forced to flow through molecular sieve beds for additional purification and removal of contaminants. Toluene (99.5%) was purchased from VETEC (Rio de Janeiro, Brazil) and was refluxed in the presence of sodium/benzophenone and distilled prior to use. EASC cocatalyst was purchased form Akzo Nobel (São Paulo, Brazil) with purity of 99% (w/v) and used as received. MAO was purchased from Akzo Nobel (São Paulo, Brazil) as a 10% aluminum (w/v) sus-

 DOI 10.1002/pen

TABLE 1. Influence of cocatalysts, polymerization temperature, and Al/Ni molar ratio on the catalyst performance and polymer average molecular weights.

Runs	Al/Ni	Temperature (°C)	Cocatalyst	Polymer yield (g)	M_w (Da)	M_n (Da)	M_w/M_n
P1	300	75	MAO	8.50	216,000	74,000	2.9
P2	300	75	EASC	9.00	na	na	na
P3	150	75	EASC	1.00	na	na	na
P4	300	45	EASC	9.00	na	na	na
P5	300	25	EASC	4.00	na	na	na
P6	300	75	DEAC	Trace	na	na	na
P7	100	75	DEAC	2.00	221,000	102,000	2.2
P8[a]	300	50	EASC	0.70	178,000	76,000	2.3
P9	300	25	DEAC	3.70	313,000	144,000	2.2
P10	300	50	DEAC	9.40	204,000	77,000	2.6

na, not available.
[a] Polymerization carried out in heptane; pressure = 1 atm.

pension and used as received. DEAC was purchased from Akzo Nobel (São Paulo, Brazil) with purity 99.8% and used as received (w/v).

Polymerization

Manipulation of chemicals was performed under nitrogen atmosphere. Polymerizations were carried out in a mechanically stirred 1-l Parr pressure reactor. The total volume of the added liquid phase was equal to 250 ml in all runs. The catalyst precursor was suspended in a small amount of toluene. The final catalyst concentration inside the reactor was equal to 0.02 mmol/l. The cocatalyst was dissolved in a small amount of toluene before cocatalyst feeding. Ethylene consumption was measured continuously with an on-line flowmeter (KOBOLD mass flowmeter, mass-2009-C2) in real time. Reagents were charged into the reactor vessel in the following order: toluene, cocatalyst, and, after reaching the desired polymerization temperature, ethylene. The stirring speed was kept at 600 rpm in all the runs. The polymerization was started by injecting the catalyst suspension into the reactor. After the specified 1 h, the reaction was halted through combination of fast cooling and fast release of the ethylene pressure. The polymer was precipitated in ethanol, washed with ethanol, and dried in a vacuum oven.

Characterization

High-temperature gel permeation chromatograph (GPC) characterization was carried out on a Water 150 CV Plus equipment, using benzene trichloride as solvent. Four columns were used [HT-3 (10^3 A), HT-4 (10^4 A), HT-5 (10^5 A), HT-6 (10^6 A)], and analyses were performed at 140°C. The calibration curve was built with monodisperse polystyrene standards. Branching frequencies were obtained through ^{13}C NMR analyses carried out in Varian Inova 300 MHz equipment. *O*-benzene dichloride/benzene-d_6 mixture was used as solvent. Analyses were performed at 90°C with concentration of 20% (w/v) in tube probes of 5 mm of diameter.

RESULTS AND DISCUSSION

Preliminary Analysis

A set of preliminary experiments was performed to evaluate the effects of cocatalyst and temperature on the polymerization reactions, as shown in Table 1. MAO, DEAC were used as cocatalysts, and it was observed that all the three analyzed cocatalysts were able to activate the nickel (α-diimine) complex for ethylene polymerization. Similar results had also been observed by Maldanis et al. [24] using a conventional Brookhart type catalyst and by Souza et al. [22] with a [η^3-methallyl-nickel-diimine]PF_6 complex. It is important to note in Table 1 that the polymer yields are approximately the same (given the experimental errors reported in Table 2) when similar experimental conditions are employed, indicating that similar activation performances are observed for all three analyzed cocatalysts (one should compare run P1 with run P2 and run P5 with run P9). This shows that MAO can be replaced by conventional alkylaluminum compounds to promote the activation of the catalyst precursor used here. (This may be very important for development of commercial polymerization processes with this catalyst, as EASC is much less expensive and much safer to handle at plant site than MAO.)

Despite the previous observations, when runs P2 and P6 (performed at higher temperatures) are compared with each other, one can observe that polymer yields can be very different, indicating that activation efficiencies of cocatalysts can depend on reaction operation conditions. Catalyst characterizations performed with UV–vis [24] and X-ray [27] spectroscopy showed that the halide can coordinate with the metal atom, increasing the stability and the activity of the catalyst. This can explain why the experiment with DEAC (run P6) produced lesser polymer

TABLE 2. Polymerization data (2^3 factorial design).

Runs	[E] (mol/l)	P (bar)	Al/Ni	Temperature (°C)	Cocatalyst	Polymer yield (g)	M_w (10^3 Da)	M_n (10^3 Da)	M_w/M_n
R1[a]	0.3	3.4	250	50	EASC	11.5 ± 2	216 ± 5	96 ± 8	2.3 ± 0.1
R2	0.2	3.4	350	30	EASC	9.5	304	124	2.5
R3	0.2	3.4	150	30	EASC	8.3	301	108	2.8
R4	0.2	3.0	350	70	EASC	12.0	116	52	2.2
R5	0.2	3.0	150	70	EASC	14.3	130	68	1.9
R6	0.4	1.8	350	30	EASC	8.0	273	121	2.3
R7	0.4	1.8	150	30	EASC	8.5	309	125	2.5
R8	0.4	5.8	350	70	EASC	40.0	154	64	2.4
R9	0.4	5.8	150	70	EASC	35.0	180	58	3.1

[a] Performed in triplicates.

than experiments performed with EASC (run P2). As EASC is a mixture of diethylaluminum chloride and ethylaluminum dichloride, it contains more halides than DEAC.

It can be observed in Table 1 that the increase of the polymerization temperature leads to the increase of the catalyst activity when EASC is the cocatalyst (compare runs P2 and P5), indicating that the active sites remain active during the polymerization at higher temperatures. The polymerizations carried out with DEAC present maximum activity at 50°C (compare runs P6, P9, and P10). This behavior is probably due to the coordination of halides to the transition metal, which is less effective with DEAC, as it contains less halides than the EASC cocatalyst [24, 27]. Other effects may also be important and the catalyst may be very sensitive to small changes of the composition of the reaction medium, as shown later. As expected for an ionic propagating species, [1] the use of an aliphatic solvent caused a dramatic decrease of the polymerization rate (compare runs P4 and P8). The increase of the Al/Ni molar ratio seems to cause the increase of the polymer yields (compare runs P2 and P3), showing that EASC is probably able to scavenge impurities from the reaction medium and to activate the Ni complex for polymerization. However, the most important piece of information in Table 1 is that the cocatalysts do not exert the same effect on catalyst activities and performances (compare runs P1, P2, and P6), although similar activities can be obtained at different conditions (compare runs 2, 3, and 16). Therefore, there are incentives to study the use of EASC as the cocatalyst of the Ni catalyst studied here.

Experimental Design

The experiments presented in Table 1 show that EASC may be an efficient cocatalyst for the activation of the Ni catalyst during ethylene polymerization. For this reason, EASC was selected as the cocatalyst for a more detailed systematic study of the reaction parameters. Table 2 shows the experimental results obtained for a 2 [3] experimental design where the independent variables were ethylene pressure, Al/Ni molar ratio, and the polymerization temperature (Table 2). Replicates of the central point were performed for evaluation of experimental variability. As shown in Table 2, reproducibility can be regarded as very good and relatively unimportant, when compared with the range of variation of analyzed process responses. The analyzed experimental responses were the polymer yield and the number and weight average molecular weights of the polymer samples. The calculated main effects of the independent variables are presented in Tables 3 and 4. These tables show the estimated parameters, the standard errors, the *t*-values, and the associated

TABLE 3. Main and interaction effects of the independent variables on polymer yield produced by the polymerization data of Table 2.

Coefficients	a_1	a_2	a_3	$a_{1,3}$	a_0
		Empirical Model with mean effects ($R = 0.82$)			
Estimate	5.97	0.376	8.34	–	15.4
Std.Err.	0.25	0.25	0.25	–	0.213
$t(7)$	23.9	1.51	33.4	–	72.3
p-level	5.72×10^{-8}	0.176	5.64×10^{-9}	–	2.54×10^{-11}
		Empirical Model with mean and interaction effect ($R = 0.96$)			
Estimate	5.97	0.376	8.34	6.29	15.4
Std.Err.	0.25	0.25	0.25	0.25	0.213
$t(7)$	23.9	1.51	33.4	25.1	72.3
p-level	3.53×10^{-7}	0.183	4.83×10^{-8}	2.61×10^{-7}	4.70×10^{-10}

Estimated parameters are: a_1 (ethylene concentration); a_2 (Al/Ni molar ratio); a_3 (temperature); $a_{1,3}$ (interception with ethylene concentration and temperature); a_0 (independent term). R represents the correlation coefficient between experimental and calculated values; $t(n)$ represents the value of the *t*-Student variable with n degrees of freedom; p-level represents the probability for the model parameter to be equal to zero.

TABLE 4. Main effects of the independent variables on molar mass (M_w and M_n) and polydispersity of polymers produced with the polymerization of Table 2.

Coefficients	a_1	a_2	a_3	a_0	$a_{1,3}$
	Empirical model for weight average molar mass (M_w) (calculated correlation $R = 0.96$)				
Estimate	8.21×10^3	-9.21×10^3	-7.59×10^4	2.20×10^5	–
Std.Err.	0.25	0.25	0.25	0.213	–
$t(7)$	3.28×10^4	-3.68×10^4	-3.03×10^5	1.03×10^6	–
p-level	6.40×10^{-30}	2.88×10^{-30}	0.00	0.00	–
	Empirical model for number average molar mass (M_n) (calculated correlation $R = 0.96$)				
Estimate	1.78×10^3	2.02×10^2	-2.97×10^4	9.24×10^4	–
Std.Err.	0.25	0.25	0.25	0.213	–
$t(7)$	7.13×10^3	8.09×10^2	-1.19×10^5	4.33×10^5	–
p-level	2.81×10^{-25}	1.16×10^{-18}	0.00	0.00	–
	Empirical model for polydispersity (calculated correlation $R = 0.84$)				
Estimate	0.115	−0.116	−0.036	2.24	0.238
Std.Err.	0.089	0.089	0.089	0.145	0.089
$t(5)$	1.30	−1.31	−0.402	15.4	2.68
p-level	0.251	0.247	0.704	2.07×10^{-5}	0.044

Estimated parameters are: a_1 (ethylene concentration); a_2 (Al/Ni molar ratio); a_3 (temperature); a_0 (independent term); a_{13} (interception with ethylene concentration and temperature). R represents the correlation coefficient between experimental and calculated values; $t(n)$ represents the value of the t-Student variable with n degrees of freedom; p-level represents the probability for the model parameter to be equal to zero.

p-levels. These values are used for computation of the statistical significance of the empirical models [28]. Figures 2–4 show the predicted and observed values for the polymer yield, weight-average molecular weights, and polydispersity, obtained from the linear models described in *Eq. 1* (Figs. 2–4).

$$y_i = a_0 + \sum_{i=1}^{n} a_i x_i + \sum_{i=1}^{n} \sum_{j=i+1}^{n} a_{ij} x_i x_j + \varepsilon_i \qquad (1)$$

In *Eq. 1*, a_0 is the independent term, x_i represents the independent polymerization variables, y_i represents model responses, and a_i and a_{ij} are model parameters (main effects and interaction effects, respectively). The parameters of the linear model were estimated with the experimental data presented in Table 2. Figures 2–4 show that there is a good agreement between predicted and experimental polymer yields, weight-average molecular weights and polydispersities. Therefore, main effect analysis can be performed with confidence. Observed mismatch between experimental and calculated polydispersities should not be overemphasized because of the relatively low variations observed in the analyzed experimental conditions.

Table 3 shows that the most important effects on the polymer yield are the ethylene concentration and the polymerization temperature. The increase of the ethylene concentration leads to the increase of the polymer yield due to the increase of the propagation rates. The increase of polymer yield with temperature could be attributed to two factors: (a) formation of additional active catalyst sites, as described by Gates et al. [29] and (b) larger activation energies for monomer propagation than for catalyst deactivation, as reported for similar MAO/Ni catalyst systems [29–31]. These effects are clearly illustrated in Fig. 5, where one can notice the higher reaction rates and the faster rate of catalyst decay at 70°C than at 50°C (see Fig. 5). In addition, Table 3 shows an important two-way

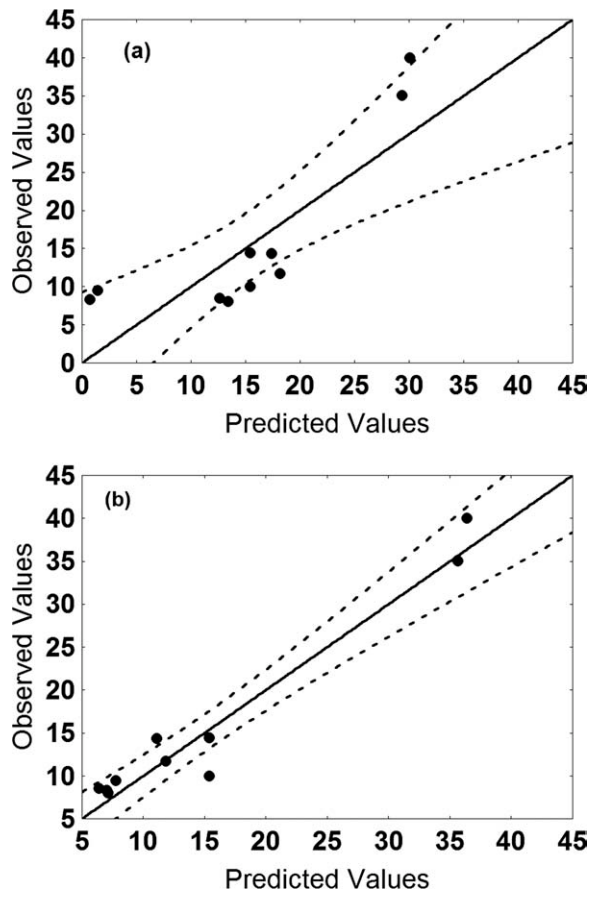

FIG. 2. Predicted vs. observed values for the polymer yield (g), (a) empirical model without interaction effect ($a_{1,3}$) and (b) empirical model with interaction effect ($a_{1,3}$; see Table 2 for experimental condition).

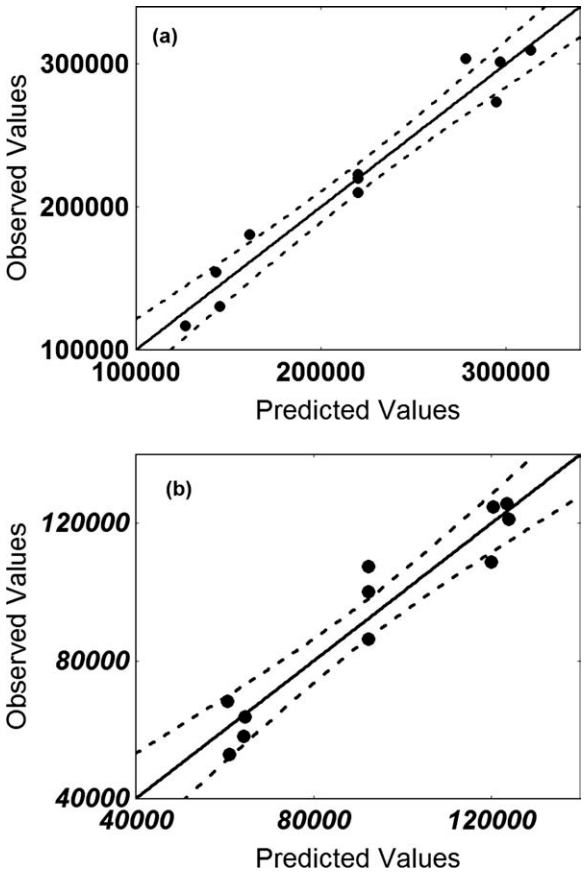

FIG. 3. Observed vs. predicted values for the number (M_n) and weight average molecular weight (M_w) (g/mol) (see Table 2 for experimental condition).

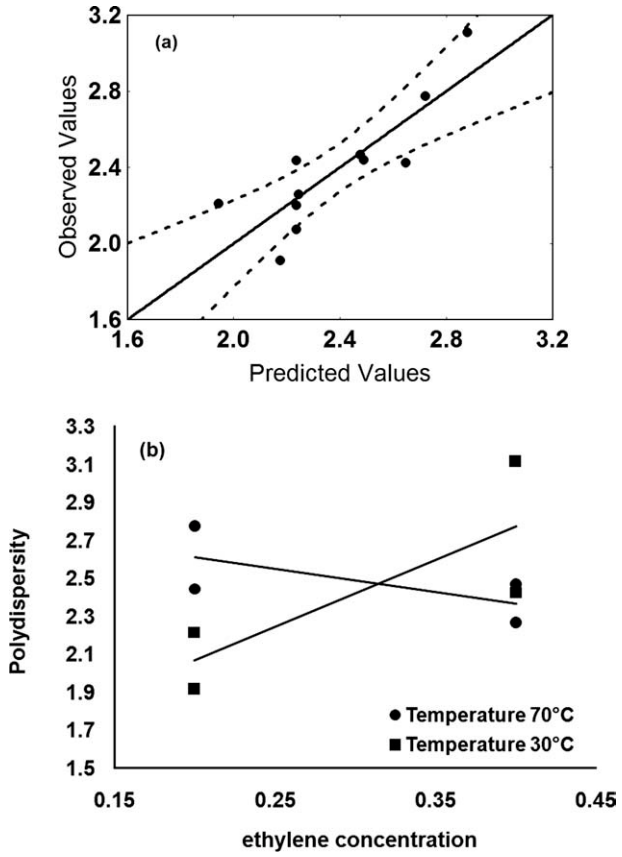

FIG. 4. (a) Observed vs. predicted values for the polydispersity of the molecular weight distribution and (b) interaction effect between ethylene concentration and temperature (see Table 2 for experimental condition).

interaction between ethylene and temperature process conditions. This behavior shows that the effect of ethylene concentration on polymer yield may depend on temperature levels, indicating the possible modification of the relative amounts of the different catalyst sites as the polymerization temperature changes.

The *t*-values and respective *p*-levels indicate that estimated parameters are statistically significant and that the polymerization temperature exerts the most important effect on the final average molecular weights of the obtained polymer samples (see Table 4) [28]. This probably indicates that chain transfer to alkylaluminum and to monomer are less important than spontaneous chain transfer in this polymerization system, suggesting that the an important chain transfer step is the β-hydride elimination, as previously reported for similar catalyst systems [12]. Table 4 also shows the existence of a two-way interaction between ethylene concentration and temperature when polydispersity is considered (although this interaction is not very strong). From Fig. 4b, it can be observed that the increase of temperature leads to the decrease of polydispersity at low ethylene concentration (0.2 mol/l). However, at high ethylene concentration (0.4 mol/l), the effect of temperature is the opposite. The effect of these variables can be explained in terms of the increase of the number of active sites, when the Al/Ni molar ratio and the reaction temperature are increased. The interaction between the ethylene concentration and temperatures and its effects on polydispersity of polymer samples have not been observed with other similar catalyst systems. It is proposed here then that the increase of temperature may

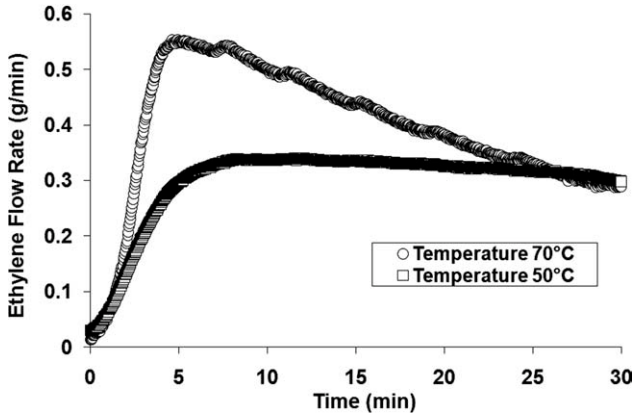

FIG. 5. Ethylene consumption rates at different temperatures (○) R1 [ethylene] = 0.3 mol/L; Al/Ni = 250; cocatalyst = EASC (□) R8 [ethylene] = 0.4 mol/L; Al/Ni = 350; cocatalyst = EASC.

DOI 10.1002/pen

TABLE 5. Branch frequencies of obtained polyethylene samples.

	P1	R2	R4	R5	R6	R7	R8	R9	R10
Methyl	23.8	21.6	21	19.4	19.5	22	24	18.9	19.4
Ethyl	4.8	3.1	2.2	2	5.7	3.7	2	2.9	4
Propyl	3.1	2.8	2.3	1	0.3	3.1	1.1	0.9	1.1
Butyl	1.7	1.3	0.7	1.6	3.3	1.3	1.2	1.5	2
Amyl	1.7	1.3	0.7	1.4	0.6	1.3	1.9	0.8	2
Long	8.3	6.4	4.9	7.1	11.8	8.6	5.6	7.7	9.4
Isobutyl	0.5	0.6	0.6	1.5	2.7	0.3	1.4	0	4.2
2Methyl-hexyl	1.1	0.5	0.6	0	0.05	0.5	0.3	0.5	0.3
Total of branches	45	37.7	33	34	43.9	40.9	37.4	33.3	42.4

See Tables 1 and 2 for information about polymerization conditions. The number of branches is represented (in mol) per mol of ethylene in the polymer—mol%.

cause a change of the relative amounts of the distinct active species during the reaction. The formation of long-chain branches through incorporation of vinyl terminated polymer chains produced by β-hydride elimination can also lead to the simultaneous increase of the average molecular weight and polydispersity when temperature increases. This was shown by Suzuki et al. [20] for a conventional Brookhart catalyst. However, available experimental data do not allow us to provide unequivocal interpretation of the experimental results at this moment.

Analysis of Branching

Branch structures were evaluated through ^{13}C NMR. The polyethylene samples obtained with this Ni catalyst present large amounts of methyl, ethyl, propyl, butyl, pentyl, and long branches with six or more carbons, as shown in Table 5. The presence of branches with one to five carbons, closely following the Flory most probable distribution, has been previously described in the literature and can be obtained through chain running [22]. In this case, a sequence of ethylene insertions and catalyst isomerizations (β-hydride elimination/reinsertion) leads to the formation of short-chain branches, as described in Fig. 6. It is important to note that this mechanism leads to a Flory distribution because of the statistical nature of the running mechanism.

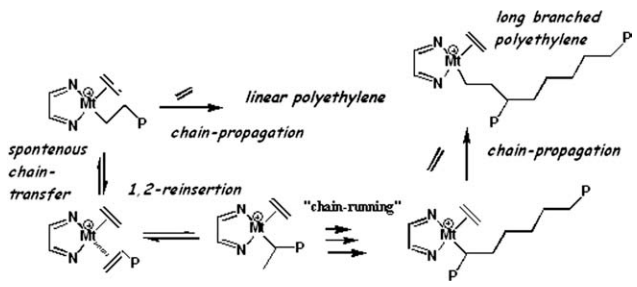

FIG. 6. Representation of the chain running mechanism for ethylene polymerization with a late metal transition catalyst.

The ^{13}C NMR analyses performed here did not allow for quantification of branches containing more than six carbons. However, the chain-running mechanism cannot be invoked to explain the high amount of long branches detected experimentally in the polymer samples. Therefore, this suggests that the appearance of long chain branches is related to macromonomer reincorporation. This hypothesis was originally proposed by Suzuki et al. for a conventional Brookhart catalyst [20]. Suzuki et al. also described the existence of multiple active catalyst sites with different reactivities for macromonomer reincorporation. Thus, it seems that the studied catalyst is able to produce both short and long branches through simultaneous chain walking and macromonomer reincorporation. Samples of the obtained ^{13}C NMR spectra may be observed in Fig. 7 (see Fig. 7). NMR peak assignments are presented in Table 6, where one can observe the presence of different types of short branches: methyl, ethyl, propyl, butyl, amyl, isobutyl, and 2-methyl hexyl (Table 6). The nomenclature used here is the one proposed by Usami and Takayama [32] for isolated branches. Branches are named as xB_n, where n represents the size of the branch and x indicates the number of carbon atoms. For the backbone carbons, greek letters and "br" are used to represent methylene carbon and a branching point, respectively (see Fig. 8 for the detailed nomenclature).

New types of branches were observed in the polyethylene samples produced with the analyzed (α-diimine) nickel catalyst, as shown in Fig. 9. These branches have not been reported previously for polyethylene samples produced with similar catalysts, although they have also been observed in our group for polypropylenes produced with the same catalyst [25]. Assignments for isobutyl branches can be found at 23.24 and 25.2 ppm, ressonances 9 and 13 on the ^{13}C NMR spectra observed in Fig. 7, corresponding to $1B_{iBu}$ and $2B_{iBu}$ carbons. Peaks placed at 27.86 and 39.51 ppm can be assigned to carbons $2B_{2MH}$ and $3B_{2MH}$, ressonances 20 and 44 in Fig. 7, of 2

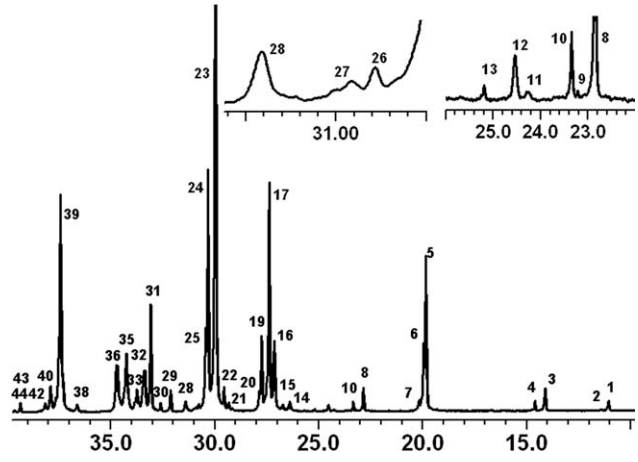

FIG. 7. ^{13}C NMR spectra of polyethylene sample obtained at R1 (see Table 2 for information about polymerization conditions).

TABLE 6. NMR peak assignments [32–36].

Peak No	Chem. shift calc (ppm)	Chem. shift [prev. works] (ppm)	Chem. shift exp. (ppm)	Assignments
1	11.36	32.01 [33], 32.209 [34]	11.10	$1B_2$
2	11.85		11.50	$1,2\text{-}1B_2$
3	13.86	14.08 [33], 14.324 [34]	14.12	$1B_4$,
		14.02 [33], 14.07 [34]		$1B_5$, $1B_n$,
				$1,4\text{-}1B_n$
4	14.35	14.0 [32], 14.59 [33]	14.65	$1B_3$
5	19.63	20.032 [1], 20.04 [33]	19.90	$1B_1$, $1,5\text{-}B_1$, $1,6\text{-}B_1$
6	19.63		19.99	$1,4\text{-}1B_1$
7	20.21	20.15 [33]	20.30	$2B_3$
8	22.65	22.8 [32], 22.88 [33]	22.88	$2B_5$
		22.84 [33], 22.88 [34]		$2B_n$
				$1,4\text{-}2B_n$
	22.13			$1B_{2MH}$
9	22.62		23.24	$1B_{iBu}$
10	22.90	23.36 [33], 23.38 [34]	23.37	$2B_4$
11	24.72		24.30	$1,2\text{-}2B_2$
12	24.58	24.65 [13], 24.85 [33]	24.61	$1,5\text{-}\beta'B_1$
13	25.92		25.20	$2B_{iBu}$
14	27.16	26.789 [34]	26.51	$2B_2$
15	27.77		26.87	$1,2\text{-}\beta B_2$
16	27.52	27.3 [32], 27.35 [34]	27.20	βB_2
		27.33 [33, 34]		βB_3, βB_4, βB_5, βB_n, $(n-1)B_n$, $1,4\text{-}\beta B_n$, $1,4\text{-}(n-1)B_n$, βB_{iBu}
17	27.27	27.45 [34]	27.42	βB_1
				$1,4\text{-}\beta B_1$, $1,5\text{-}\beta B_1$, $1,6\text{-}\beta B_1$,
		27.3 [32]		$4B_5$
18	27.77			$4B_{2MH}$, $5B_{2MH}$
19	27.52	27.85 [32]	27.79	$1,6\text{-}\beta'B_1$
20	27.99		27.86	$2B_{2MH}$
21	29.96	29.55 [13]	29.38	$3B_4$
22	29.71	29.536 [13]	29.59	$4B_n$
				$1,4\text{-}4B_n$
23	29.96	30.00 [33, 34]	30.00	δB_{1-n}
24	30.21	30.38 [34]	30.36	γB_1
				$1,4\text{-}\gamma B_1$, $1,5\text{-}\gamma B_1$, $1,6\text{-}\gamma B_1$
25	30.21	30.50 [34]	30.48	γB_2, γB_4
				γB_3, γB_5, $1,4\text{-}\gamma B_n$, $1,4\text{-}(n-2)B_n$, $1,2\text{-}\gamma B_2$, γB_{iBu}
		30.476 [13]		γB_n
26	30.46		30.79	$1,7\text{-}\gamma B_{1-n}$
27	31.78		30.90	$1,2\text{-}\alpha B_2$
28	32.03		31.50	$1.4\text{-}\alpha'B_n$
29	32.40	32.232 [1], 32.18 [33]	32.16	$3B_n$
				$1,4\text{-}3B_n$
30	32.65	32.8 [32], 32.70 [33]	32.65	$3B_5$
31	32.52	33.32 [2], 33.26 [34]	33.14	brB_1
				$1,5\text{-}brB_1$, $1,6\text{-}brB_1$
32	32.52		33.409, 33.476, 33.543	$1,4\text{-}brB_1$
33	34.22	34.328 [13], 34.13 [34]	33.83	αB_2
34	34.22	34.22 [33],34.20 [34]	33.94	$4B_4$
35	34.47		34.39	αB_3
		34.60 [34]		αB_4
		34.7 [32]		$5B_5$
		34.7 [32], 34.61 [33]		αB_5, αB_n, nB_n
				$1,4\text{-}\alpha B_n$, $1,4\text{-}nB_n$
				$6B_{2MH}$
	34.72			αB_{iBu}
36	34.22	$r - 35.7/m - 34.9$ [32]	34.731, 34.785	$1,4\text{-}\alpha'B_1$
37	34.98			brB_{iBu}
38	36.91		36.72	$3B_3$
39	36.91	37.56 [34]	37.47	αB_1
				$1,4\text{-}\alpha B_1$, $1,5\text{-}\alpha B_1$,
				$1,6\text{-}\alpha B_1$, $1,6\text{-}\alpha'B_1$

DOI 10.1002/pen

TABLE 6. (*Continued*).

Peak No	Chem. shift calc (ppm)	Chem. shift [prev. works] (ppm)	Chem. shift exp. (ppm)	Assignments
40	37.05	$r - 38.8/m - 37.96$ [32]	37.8	brB_3
	37.16			1,5-$\alpha'B_1$
41	37.05	38.23 [33], 38.19 [34]	37.99	brB_4
		38.23 [33]		brB_5
		38.23 [33, 38.24 [34]		brB_n
				brB_{2MH}
42	37.05		38.24	1,4-brB_n
43	39.12	39.75 [33, 34]	39.44	brB_2
44	39.35		39.51	$3B_{2MH}$
45	41.59			1,2-brB_2
46	43.86			$3B_{iBu}$

methyl-hexyl branches. $1,2B_2$ branches are present in the produced polyethylenes, as confirmed by assignments 1,2-$1B_2$ and 1,2-$2B_2$, corresponding to peaks placed at 11.50 and 24.30 ppm (ressonances 2 and 11 in Fig. 7). Additional confirmation can be obtained with peaks placed at 26.87 ppm (assignment 15 in Fig. 7) and 30.9 ppm (assignment 44 in Fig. 6), corresponding to 1,2-βB_2 and 1,2-αB_2 carbons, respectively. The interested reader should refer to the literature for additional information about NMR peak assignment and interpretation [32–36].

Table 7 shows the empirical models based on the effect of polymerization variables on the formation of the different branch types (Table 7). Variable effects were calculated with the help of *Eq. 1*. It can be observed in Table 7 that the reaction temperature exerts significant influence on all analyzed variables. However, the effect of temperature is more important on the formation of methyl, ethyl, long, and total branches along the polymer chain. The importance of the reaction temperature for formation of branches has already been reported for other similar catalyst systems [29–31]. Increase of the reaction temperature promotes the increase of the relative short and long-chain branch formation, indicating that the spontaneous chain transfer is the main mechanism that controls molar masses and that chain-running steps competes with chain propagation, as described in Fig. 6. This is confirmed by the decrease of the molecular weight averages when the polymerization temperature increases.

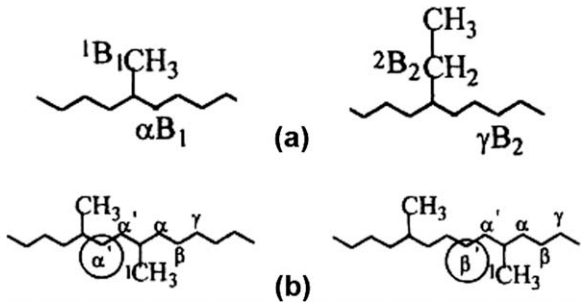

FIG. 8. Nomenclature utilized to characterize carbons of polyethylene samples.

The temperature effect is followed by the effect of the Al/Ni molar ratio, which exerts significant influence on the formation of 1,2-B_2 branch. The influence of Al/Ni molar ratio indicates that these branches probably are not formed only through chain-running. In addition, the isobutyl branch is influenced by the Al/Ni molar ratio, although an interaction effect between the Al/Ni molar and temperature can be observed. This result shows that the dominant mechanism to obtain the isobutyl braches is not the chain-running, indicating that the effect of Al/Ni molar ratio on isobutyl braches depend on the temperature level. This behavior is not usual and it is possible that the EASC cocatalyst takes part on the mechanism that leads to isobutyl branch formation. The long branch frequencies are influenced more significantly by the temperature than by any other parameter. This seems to indicate that the macromonomer reincorporation could explain the significant amount of long branches. In this case, the higher temperature leads to an increase of the macromonomer concentration, which is reincorporated by growing polymer chains.

Simple Kinetic Modeling

On the basis of the main effect analysis performed in the previous section, a more detailed kinetic model was developed and implemented. A simple semiempirical phenomenological model was implemented to allow for preliminary evaluation of kinetic rate constants of the most important mechanistic effects (as described previously), based on the available rates of monomer consumption, as

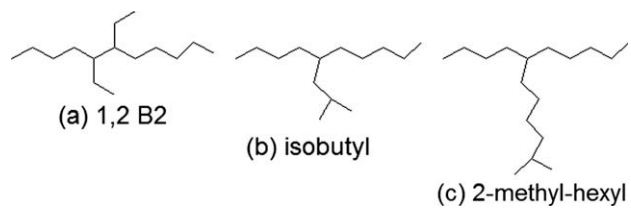

FIG. 9. New types of polyethylene branches obtained with the analyzed (α-diimine) nickel catalyst.

TABLE 7. Empirical models of polymerization variables on branch frequencies.

Coefficients	a_0	a_1	a_2	a_3	$a_{1,2}$	$a_{1,3}$	$a_{2,3}$
			Empirical model for methyl branch ($R = 0.92$)				
Estimate	20.5	−0.150	0.650	1.20	0.875	−0.775	−1.03
Std. Err.	0.533	0.462	0.462	0.462	0.462	0.462	0.462
$t(2)$	38.5	−0.325	1.41	4.58	1.89	−1.68	−2.22
p-level	6.74×10^{-4}	0.776	0.295	0.039	0.199	0.235	0.157
			Empirical model for ethyl branch ($R = 0.99$)				
Estimate	3.03	−0.200	0.275	0.925	−0.275	−0.375	0.450
Std. Err.	0.033	0.029	0.029	0.029	0.029	0.029	0.029
$t(2)$	91.0	−6.93	9.53	32.0	−9.53	−13.0	15.6
p-level	1.21×10^{-4}	2.02×10^{-2}	1.08×10^{-2}	9.73×10^{-4}	1.08×10^{-2}	5.87×10^{-3}	4.09×10^{-3}
			Empirical model for long branch ($R = 0.99$)				
Estimate	6.13	−0.450	0.275	1.33	0.025	−0.775	1.35
Std. Err.	0.133	0.115	0.115	0.115	0.115	0.115	0.115
$t(2)$	46.0	−3.90	2.38	11.5	0.217	−6.71	11.7
p-level	4.72×10^{-4}	6.00×10^{-2}	0.140	7.51×10^{-3}	0.849	2.15×10^{-2}	7.24×10^{-3}
			Empirical model for isobutyl branch ($R = 0.99$)				
Estimate	0.667	0.608	0.950	0.400	0.575	0.175	0.825
Std. Err.	0.033	0.029	0.029	0.029	0.029	0.029	0.029
$t(2)$	20.0	13.8	32.9	13.9	19.9	6.06	28.6
p-level	2.49×10^{-3}	5.21×10^{-3}	9.22×10^{-4}	5.17×10^{-3}	2.51×10^{-3}	2.61×10^{-2}	1.22×10^{-3}
			Empirical model for $1,2B_2$ branch ($R = 0.99$)				
Estimate	0.287	-2.50×10^{-3}	0.153	0.250	−0.025	0.023	0.078
Std. Err.	0.019	0.016	0.016	0.016	0.016	0.016	0.016
$t(2)$	15.4	−0.156	9.49	15.6	−1.56	1.40	4.82
p-level	4.17×10^{-3}	0.891	1.09×10^{-2}	4.11×10^{-3}	0.260	0.297	4.04×10^{-2}
			Empirical model for total branch ($R = 0.99$)				
Estimate	37.9	−0.550	1.78	2.97	1.28	−1.48	1.00
Std. Err.	0.100	0.087	0.087	0.087	0.087	0.087	0.087
$t(2)$	379	−6.35	20.5	34.4	14.7	−17.0	11.5
p-level	6.96×10^{-6}	2.39×10^{-2}	2.37×10^{-3}	8.46×10^{-4}	4.58×10^{-3}	3.43×10^{-3}	7.42×10^{-3}

Estimated parameters are: a_1 (ethylene concentration); a_2 (Al/Ni molar ratio); a_3 (temperature); $a_{1,2}$ (interception with ethylene concentration and A/Ni molar ratio); $a_{1,3}$ (interception with ethylene concentration and temperature); $a_{2,3}$ (interception with Al/Ni molar ratio and temperature; a_0 (independent term). R represents the correlation coefficient between experimental and calculated values; $t(n)$ represents the value of the t-Student variable with n degrees of freedom; p-level represents the probability for the model parameter to be equal to zero.

described by Matos et al. [37–39] *Eqs. 2–5* describe the simplified mechanism used for interpretation of available experimental data.

$$\mathrm{Cat}_i + \mathrm{Cocat} \xrightarrow{\mathrm{Katvi}} \mathrm{cat}_i^{\mathrm{o}} \tag{2}$$

$$\mathrm{Cat}_i^{\mathrm{o}} + \mathrm{M} \xrightarrow{\mathrm{Kpi}} \mathrm{Pol} + \mathrm{Cat}_i^{\mathrm{o}} \tag{3}$$

$$\mathrm{Cat}_i^{\mathrm{o}} \xrightarrow{\mathrm{Kdi}} \mathrm{Cat_d} \tag{4}$$

$$\mathrm{Cat}_i \xrightarrow{\mathrm{Kdi}} \mathrm{Cat_d} \tag{5}$$

where Cat_i represents a potential catalyst site of type i; Cocat represents the cocatalyst; $\mathrm{Cat}_i^{\mathrm{o}}$ is the activated catalyst of type i; M is the monomer species; $\mathrm{Cat_d}$ is the deactivated catalyst; and Katvi, Kpi, and Kdi are kinetic rate constants for site activation, propagation, and deactivation for catalyst site of type i, respectively. On the basis of the proposed mechanism, the following set of mass balance equations can be written:

$$\frac{d\mathrm{Cat_i}}{dt} = -\mathrm{Katv}_i \mathrm{Cocat}\ \mathrm{Cat}_i$$

$$\mathrm{Cat_i}(t) = \mathrm{Cat}_i(0)\exp(-\mathrm{Katv}_i\ \mathrm{Cocat}\ t) \tag{6}$$

$$\frac{d\mathrm{Cat_i^o}}{dt} = \mathrm{Katv}_i\ \mathrm{Cocat} - \mathrm{Kd}\ \mathrm{Cat}_i^{\mathrm{o}}$$

$$\mathrm{Cat}_i^{\mathrm{o}}(t) = \mathrm{Cat}_i^{\mathrm{o}}(0)[\exp(-\mathrm{Kd}_i\ t) - \exp(-\mathrm{Katv}_i\ \mathrm{Cocat}\ t)] \tag{7}$$

$$\mathrm{Rate}(t) = \sum_{i=1}^{\mathrm{N}} Kp_i f_i M\, \mathrm{Cat}_i^{\mathrm{o}}$$

$$= \sum_{i=1}^{\mathrm{N}} Kp_{\mathrm{i}} f_i M\{\mathrm{Cat}_i^{\mathrm{o}}(0)[\exp(-\mathrm{kd}_i t) - \exp(-\mathrm{Katv}_i\, \mathrm{Cocat}\, t)]\} \tag{8}$$

where f_i represents the relative concentration of catalyst site i in the catalyst mixture. Assuming that the monomer concentration remains constant throughout the batch and

 DOI 10.1002/pen

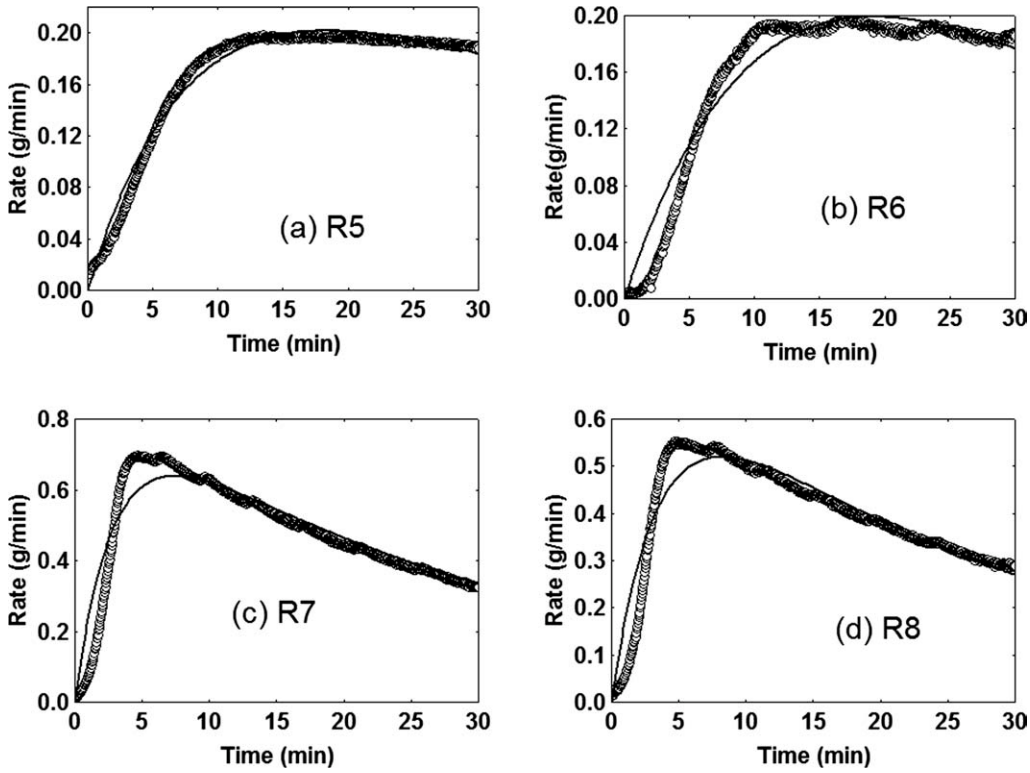

FIG. 10. Model fitting of available rate data with EASC cocatalyst (R5 − [ethylene] = 0.2 mol/L; Al/Ni = 150; Temperature = 70°C; R6 − [ethylene] = 0.4 mol/L; Al/Ni = 350; Temperature = 30°C; [ethylene] = 0.4 mol/L; Al/Ni = 150; Temperature = 30°C; [ethylene] = 0.4 mol/L; Al/Ni = 350; Temperature = 70°C).

that activation and deactivation rate constants are similar for all catalyst sites, *Eq. 8* can be rewritten as:

$$\text{Rate} = \frac{A}{\text{Kd}}\{[\exp(-\text{Kd}\,t) - \exp(-\text{Katv Cocat}\,t)]\} \quad (9)$$

where A, Kd and Katv are the parameters that must be estimated. Figure 10 illustrates the obtained model fitting at different reaction conditions (see Fig. 10). As the simple model provides very good fitting of the experimental rate data, it may be assumed that a single catalyst site is probably present in the catalyst system, as it might be already expected. (The initial mismatch between model predictions and experimental data is probably related to mixing of catalyst inside the reaction vessel or more complex catalyst initiation.) This means that the large polydispersities presented in Table 2 and within the range 2.2–3.1 may originate from varying reaction conditions or macromonomer reincorporation, as discussed previously and indicated by the long chain frequencies. Parameter estimates are presented in Table 8 and indicate that the rates of catalyst decay and catalyst activation may be very different at distinct polymerization conditions (Table 8). Table 8 shows that lower temperatures lead to lower kinetic constants. These results can be clearly observed in the Fig. 10. Therefore, the observed polymer yields and polymer properties depend on the activation energies of the distinct mechanistic steps. As catalyst activation is not instantaneous, this step should not be neglected during more involving analysis of the kinetic data.

CONCLUSIONS

This work analyzed the effects of some polymerization variables (ethylaluminum sesquichoride concentration, polymerization temperature, ethylene concentration) on the polymer yields, average molecular weights, and relative frequencies of short and long branches of polyethylene samples prepared with a (α-diimine) nickel catalyst. It was shown that the polymerization temperature is the most important variable in this system, exerting strong influences in all analyzed process responses. Formation of short chain branches was observed experimentally and probably results from chain running. New types of short

TABLE 8. Estimated parameters for different runs (see Table 2 for reaction conditions).

Runs	R5	R6	R7	R8
A (g/min)	0.0346	0.2029	0.2891	0.0939
Katv (min^{-1})	0.1083	0.2539	0.3218	0.1204
Kd (min^{-1})	0.0171	0.0361	0.0328	0.0081
R^2	0.99	0.95	0.95	0.97

See Table 2 for experimental conditions. Model parameters were estimated with the least-squares technique, with the help of the Newton optimization procedure [39].

branches (1,2B_2, isobuytl and 2-methyl-hexyl) were detected in the obtained polyethylene samples, although the mechanisms that lead to formation of these branches are not clear yet. Particularly, formation of isobutyl branches is strongly influenced by the EASC concentration, indicating that chain transfer to EASC may take part of the branch formation. Long-chain branches were also observed in the produced polymer samples, indicating that macromonomer reincorporation can also occur with the analyzed catalyst system. Finally, a simple mechanistic model was proposed and used to interpret available rate data, indicating that rates of catalyst activation and catalyst decay depend strongly on the polymerization conditions. However, as obtained fits are always good when a single catalyst site is assumed to exist, it may be considered that a single catalyst site is produced during catalyst activation and that the large polydispersities result from varying reaction conditions and/or macromonomer reincorporation, as observed experimentally.

REFERENCES

1. P. Galli and G. Vecellio, *Prog. Polym. Sci*., **26**, 1287 (2001).
2. H.H. Brintzinger, D. Fisher, R. Mulhaupt, B. Rieger, and R.M. Waymouth, *Chem. Rev*., **34**, 1143 (1995).
3. R.A. Bubeck, *Mater. Sci. Eng. R*, **39**, 1 (2002).
4. M.C. Forte, M.S.L. Miranda, and J. Dupont, *Polímeros: Ciência e Tecnologia*, **6**, 3, 49 (1996).
5. E. Kolodka, W.J. Wang, P.A. Charpentier, S. Zhu, and A.E. Hamielec, *Macromolecules*, **35**, 10062 (2002).
6. D. Beigzadeh, J.B.P. Soares, and T.A. Duever, *Macromol. Rapid Commun*., **20**, 541 (1999).
7. D. Beigzadeh, J.B.P. Soares, and T.A. Duever, *J. Polym. Sci. Part A: Polym. Chem*., **42**, 3055 (2004).
8. D. Beigzadeh, J.B.P. Soares, and A.E. Hamielec, *J. Appl. Polym. Sci*., **71**, 1753 (1999).
9. E. Kolodka, W.J. Wang, S. Zhu, and A.E. Hamielec, *Macromol. Rapid Commun*., **24**, 311 (2003).
10. A. Malmberg, J. Liimatta, A. Lehtinen, and B. Lofgren, *Macromolecules*, **32**, 6687 (1999).
11. A. Malmberg, C. Gabriel, T. Steff, H. Munsted, and B. Lofgren, *Macromolecules*, **35**, 1038 (2002).
12. C. Carlini, M. Isola, V. Liuzzo, A.M.R. Galletti, and G. Sbrana, *Appl. Catal. A*, **231**, 307 (2002).
13. P. Preishuber-Pflugl and M. Brookhart, *Macromolecules*, **35**, 6074 (2002).
14. S.D. Ittel, L.K. Johnson, and M. Brookhart, *Chem. Rev*., **100**, 1169 (2000).
15. G. Melillo, L. Izzo, M. Zinna, C. Tedesco, and L. Oliva, *Macromolecules*, **35**, 9256 (2002).
16. S. Mecking, *Angew. Chem. Int. Ed*., **40**, 534 (2001).
17. H.P. Chen, Y.H. Liu, S.M. Peng, and S.T. Liu, *Organometallics*, **22**, 4893 (2003).
18. S. Matsui, Y. Inoue, and T. Fujita, *J. Synth. Org. Chem. Jpn*., **59**, 232 (2001).
19. G.J.P. Britovsek, V.C. Gibson, O.L. Hoarau, S.K. Spitzmesser, A.J.P. White, and D.J. Williams, *Inorg. Chem*., **42**, 3454 (2003).
20. N. Suzuki, J. Yu, Y. Masubuchi, A. Horiuchi, and W. Wakatsuki, *J. Polym. Sci. A: Polym. Chem*., **41**, 293 (2003).
21. B.L. Small and M. Brookhart, *Macromolecules*, **32**, 2120 (1999).
22. R.F. Souza and O.L. Casagrande Jr., *Macromol. Rapid Commun*., **22**, 1293 (2001).
23. S.A. Svejda and M. Brookhart, *Organometallics*, **18**, 65 (1999).
24. R.J. Maldanis, J.S. Wood, A. Chandrasekaran, M.D. Raush, and J.C.W. Chien, *J. Organomet. Chem*., **645**, 158 (2002).
25. G.L. Crossetti, M.L. Dias, and B.T. Queiroz, *Appl. Organomet. Chem*., **18**, 331 (2004).
26. L.C. Ferreira Jr., M. Nele, G.L. Crossetti, P.A. Melo Jr., and J.C. Pinto, *DECHEMA Monographs*, **138**, 261 (2004).
27. H.K. Luo, Z.H. Yang, B.Q. Mao, D.S. Yu, and R.G. Tang, *J. Mol. Catal. A*, **177**, 195 (1999).
28. D.C. Montgomery and G.C. Runger, *Applied Statistics and Probability for Engineers*, *4th ed*., Wiley, New York (2007).
29. D.P. Gates, S.A. Svejda, E. Oate, C.M. Killian, L.K. Johnson, P.S. White, and M. Brookhart, *Macromolecules*, **33**, 2320 (2000).
30. R.F.S. Souza, L.C. Simon, and M.C.M. Alves, *J. Catal*., **214**, 165 (2003).
31. L.C. Simom, C.P. Williams, J.B.P. Soares, and R.F. Souza, *Chem. Eng. Sci*., **56**, 4181 (2001).
32. T. Usami and S. Takayami, *Macromolecules*, **17**, 1756 (1984).
33. L.C. Simon, R.S. Mauler, and R.F. Souza, *J. Polym. Sci. Part A: Polym. Chem*., **37**, 4656 (1999).
34. L.P. Linderman and N.O. Adams, *Anal. Chem*., **43**, 1245 (1971).
35. M. De Pooter, P.B. Smith, K.K. Dohrer, K.F. Bennett, M.D. Meadows, C.G. Smith, H.P. Schouwenaars, and R.A. Geerdars, *J. Appl. Polym. Sci*., **42**, 399 (1991).
36. G.B. Galland, R.F. Souza, R.S. Mauler, and F.F. Nunes, *Macromolecules*, **32**, 1620 (1999).
37. V. Matos, A.G. Mattos Neto, and J.C. Pinto, *J. Appl. Polym. Sci*., **79**, 2076 (2001).
38. V. Matos, A.G. Mattos Neto, M. Nele, and J.C. Pinto, *J. Appl. Polym. Sci*., **86**, 3226 (2002).
39. V. Matos, M. Moreira, A.G. Mattos Neto, P.A. Melo, J.C. Pinto, *Macromol. React. Eng*., **1**, 137 (2007).